Effects of Donor Unit and π-Bridge on Photovoltaic Properties of D–A Copolymers Based on Benzo[1,2-*b*:4,5-*c*′]-dithiophene-4,8-dione Acceptor Unit

Haijun Bin,[1,2] Lu Xiao,[2] Yong Liu,[1] Ping Shen,[1,2] Yongfang Li[2]

[1]College of Chemistry and Key Laboratory of Environmentally Friendly Chemistry and Applications of Ministry of Education, Xiangtan University, Xiangtan 411105, People's Republic of China
[2]CAS Key Laboratory of Organic Solids, Institute of Chemistry, Chinese Academy of Sciences, Beijing 100190, People's Republic of China
Correspondence to: P. Shen (E-mail: shenping802002@163.com) or Y. Li (E-mail: liyf@iccas.ac.cn)

Received 14 February 2014; accepted 6 April 2014; published online 29 April 2014
DOI: 10.1002/pola.27209

ABSTRACT: A series of donor-π-acceptor (D-π-A) conjugated copolymers (**PBDT-AT, PDTS-AT, PBDT-TT**, and **PDTS-TT**), based on benzo[1,2-*b*:4,5-*c*′]dithiophene-4,8-dione (BDD) acceptor unit with benzodithiophene (BDT) or dithienosilole (DTS) as donor unit, alkylthiophene (AT) or thieno[3,2-*b*]thiophene (TT) as conjugated π-bridge, were designed and synthesized for application as donor materials in polymer solar cells (PSCs). Effects of the donor unit and π-bridge on the optical and electrochemical properties, hole mobilities, and photovoltaic performance of the D-π-A copolymers were investigated. PSCs with the polymers as donor and $PC_{70}BM$ as acceptor exhibit an initial power conversion efficiency (PCE) of 5.46% for **PBDT-AT**, 2.62% for **PDTS-AT**, 0.82% for **PBDT-TT**, and 2.38% for **PDTS-TT**. After methanol treatment, the PCE was increased up to 5.91%, 3.06%, 1.45%, and 2.45% for **PBDT-AT, PDTS-AT, PBDT-TT**, and **PDTS-TT**, respectively, with significantly increased FF. The effects of methanol treatment on the photovoltaic performance of the PSCs can be ascribed to the increased and balanced carrier transport and the formation of better nanoscaled interpenetrating network in the active layer. The results indicate that both donor unit and π-bridge are crucial in designing a D-π-A copolymer for high-performance photovoltaic materials. © 2014 Wiley Periodicals, Inc. J. Polym. Sci., Part A: Polym. Chem. **2014**, *52*, 1929–1940

KEYWORDS: benzo[1,2-b:4,5-*c*′]-dithiophene-4,8-dione; π-bridge; D-π-A copolymers; photovoltaic properties; polymer solar cells

INTRODUCTION During the past decade, polymer solar cells (PSCs) have been extensively investigated owing to their light weight, flexibility, and potentially inexpensive manufacturing.[1] The most successful PSCs to date are based on the bulk heterojunction (BHJ) devices formed from a blend of polymeric electron donor and fullerene derivative electron acceptor such as [6,6]-phenyl-C_{61}-butyric acid methyl ester ($PC_{60}BM$) or [6,6]-phenyl-C_{71}-butyric acid methyl ester ($PC_{70}BM$).[2] A persistent challenge in the development of polymer based donors has been fine-tuning of various structural and electronic features in order to maintain wide-ranging optical absorption profiles, the appropriate energy levels, high charge-carrier mobilities, solution processability, large absorption coefficients, and a favorable blend morphology.[1] Low bandgap conjugated polymers with electron donor–acceptor (D–A) architecture are particularly attractive, because of the facile tunability of their absorption bands, highest occupied molecular orbital (HOMO)/lowest unoccupied molecular orbital (LUMO) energy levels, and charge carrier mobilities by intramolecular charge transfer (ICT) from donor to acceptor moieties.[3] The power conversion efficiencies (PCEs) of the PSCs based on a number of D–A copolymers have reached up to 7%–9%.[4]

To further manipulate stereo-structure and optoelectronic properties of conjugated copolymers, some π-conjugated bridges, typically thiophene or alkylthiophene (AT) unit, were inserted between donor (D) and acceptor (A) moieties to produce D-π-A type conjugated copolymers.[5] Many efforts have been devoted to the design and synthesis of new D and A building blocks to obtain efficient copolymers for PSCs.[3,4] But there are only a few studies that focus on the π-conjugated bridges between D and A moieties.[6] π-Conjugated bridges crucially influence the electronic structure of polymer main chain and the interaction between D and A units; therefore, they remarkably affect stereo-structure and consequently photophysical, electrochemical, charge transport, and photovoltaic properties of the D-π-A

Additional Supporting Information may be found in the online version of this article.

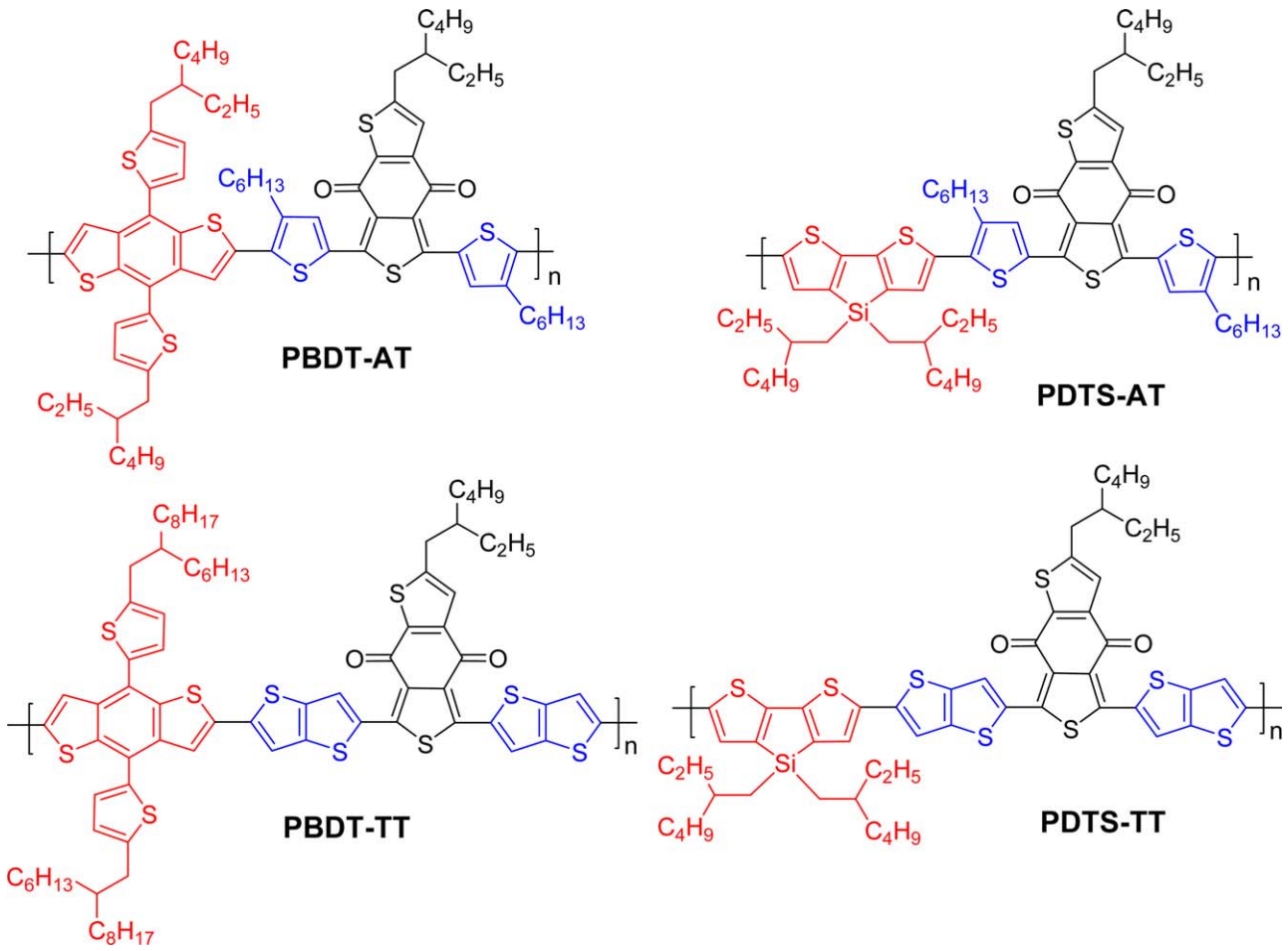

FIGURE 1 Chemical structures of the four D-π-A copolymers. [Color figure can be viewed in the online issue, which is available at wileyonlinelibrary.com.]

conjugated copolymers. In fact, the three parts in D-π-A type copolymers are very important in designing high-performance polymer photovoltaic materials. Thus, it is of prime importance to fully explore the effects of the donor units along with π-bridges on the physicochemical and photovoltaic properties in the design of new polymers for efficient PSCs. Recently, Li and Hou et al. reported a series of D-π-A copolymer with different π-bridges.[6a,e,f,g] The results showed that the π-bridges significantly affect the molecular architecture and optoelectronic properties of the copolymers.

Benzodithiophene (BDT) and dithienosilole (DTS) are attractive for the donor units in D-π-A copolymers due to their good electron-donating ability and planar molecular structure. The D–A copolymers based on BDT or DTS donor unit show broad absorption, relatively low-lying HOMO energy level, and high hole mobility, which are desirable for obtaining high-performance PSCs. Moreover, many researchers have demonstrated that AT-substituted BDT unit is a better donor unit in constructing high-performance copolymers in comparison with its alkoxyl-substituted counterpart.[7] In previous reports, thiophene or AT units are mainly used as π-bridges in D-π-A copolymers with excellent photovoltaic properties. Recently, the thieno[3,2-*b*]thiophene (TT) unit was used as the π-bridge to build D-π-A copolymers. These copolymers showed high-hole mobility in field-effect transistor[8] and PCE over 5% in PSCs.[6f,g,i,8a] The reason is TT had a rigid and coplanar fused ring which ensures a highly delocalized π-electron system and strong intermolecular π–π stacking.

As for the acceptor unit in the D–A copolymers, benzo[1,2-*b*:4,5-*c*']-dithiophene-4,8-dione (BDD)[9] and its isomer benzo[1,2-*c*:4,5-*c*']dithiophene-4,8-dione[10] unit have attracted interests due to their strong electron-withdrawing ability and fine chemical–structural modification. Some polymers based on these two acceptor units exhibited attractive and interesting properties in optoelectronic devices.[9,10] Zhu et al. reported low bandgap D–A copolymers with BDD as an acceptor unit and BDT and DTS as donor units. PSCs based on BDT–BDD copolymer gave a medium PCE of 2.18% due to its relatively narrow absorption. However, the PSC based on the DTS–BDD copolymer showed a good PCE up to 4.33% along with a high open-circuit voltage (V_{oc}, ~0.9 V), indicating that BDD is a potential building block for highly efficient conjugated polymer donors.[9] The results inspire us to insert a π-conjugated bridge between the BDT or DTS donor unit and BDD acceptor unit, which could provide an opportunity to tune the stereo-structure and optoelectronic

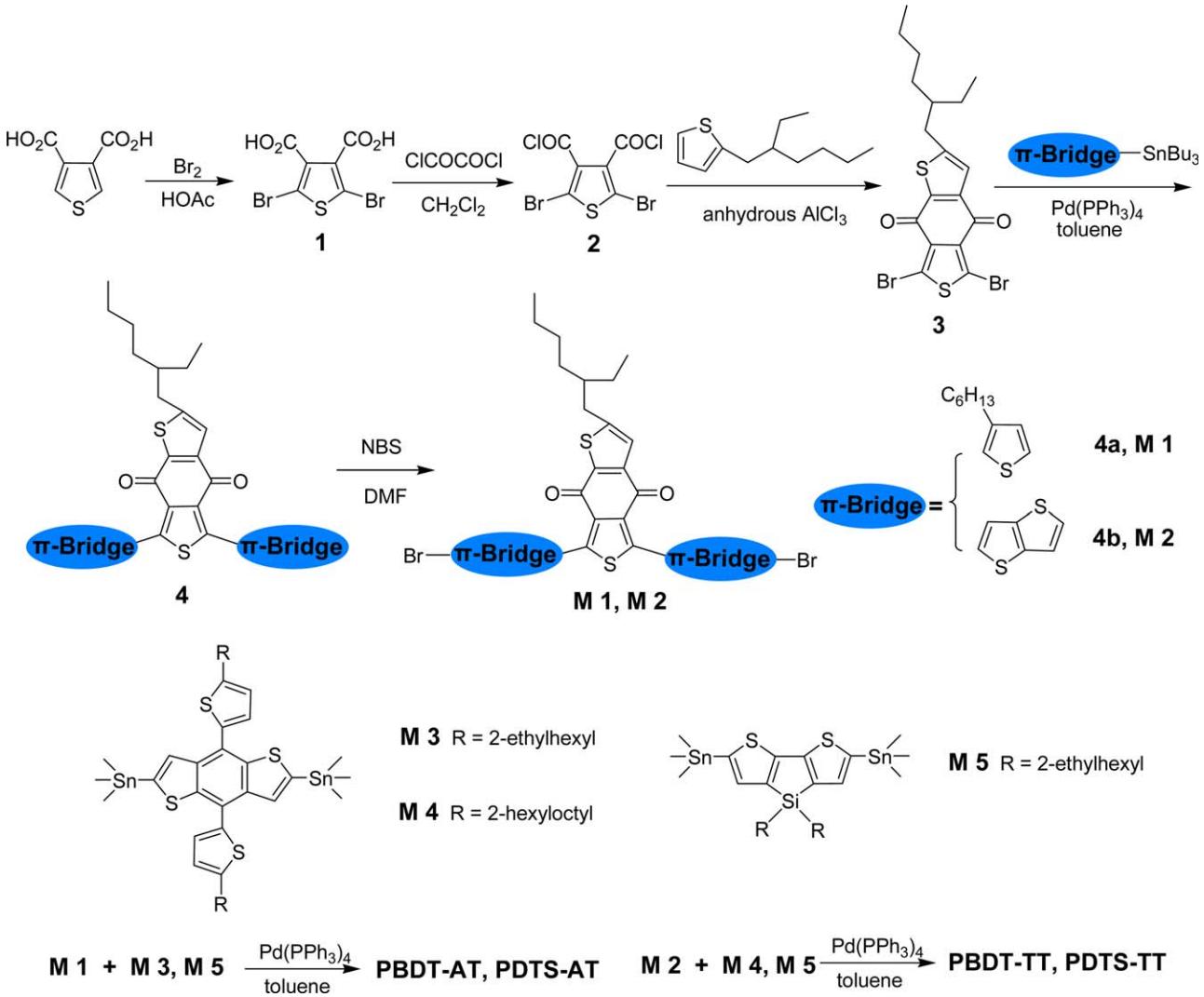

SCHEME 1 Synthetic routes of monomers and the four copolymers. [Color figure can be viewed in the online issue, which is available at wileyonlinelibrary.com.]

properties of the resulting polymers, which is expected to improve the photovoltaic performance.

Based on the above consideration, here, we designed and synthesized a series of new D-π-A copolymers (**PBDT-AT, PDTS-AT, PBDT-TT**, and **PDTS-TT**), with BDT or DTS as donor unit, AT or TT as π-bridge, and benzodithiophene-4,8-dione (BDD) as acceptor unit, as shown in Figure 1. The aim of inserting π-conjugated bridges between the D and A moieties is to tune the stereo-structure and broaden the absorption of the resulting copolymers. The effects of the different donor and π-bridge upon the optical, electrochemical properties, hole mobilities, and photovoltaic performance of the resulting copolymers were investigated.

RESULTS AND DISCUSSION

Synthesis and Characterization

The chemical structures and synthetic routes of monomers and the four D-π-A polymers are outlined in Figure 1 and Scheme 1, respectively. Thiophene-3,4-dicarboxylic acid was brominated with bromine in acetic acid to give 2,5-dibromothiophene-3,4-dicarboxylic acid (compound **1**) in a good yield (75%). Treating compound **1** with excess oxalyl chloride gave the intermediate 2,5-dibromothiophene-3,4-dicarbonyl dichloride (compound **2**). This compound was directly used in the next step without further purification. Then an important compound **3** based on BDD was obtained by a Friedel–Crafts reaction between compound **2** and 2-(2-ethylhexyl)thiophene in presence of $AlCl_3$ with 12.9% yield. Next, the BDD-based compound reacted with AT and TT, respectively, to afford compounds **4a** and **4b** via a Stille coupling reaction. The bridges of AT and TT containing monomers **M1** and **M2** were produced by bromination of **4a** and **4b** with NBS, respectively. The BDT- and DTS-based monomers (**M3, M4**, and **M5**) were prepared according to the literature methods.[7b,11] The four D-π-A copolymers **PBDT-AT, PDTS-AT, PBDT-TT**, and **PDTS-TT** were all synthesized by the palladium-catalyzed Stille-coupling polymerization. Crude copolymers were purified by extracting with methanol,

TABLE 1 Molecular Weights and Thermal Properties of the Copolymers

Copolymer	Yield (%)	M_n (kDa)[a]	M_w (kDa)[a]	PDI	T_d (°C)[b]
PBDT-AT	80	17.9	103.2	5.76	295
PDTS-AT	40	21.6	34.0	1.57	325
PBDT-TT	69	4.5	6.2	1.38	350
PDTS-TT	35	8.7	16.7	1.94	294

[a] Determined by GPC in THF based on polystyrene standards.

[b] Decomposition temperature, determined by TGA in nitrogen, based on 5% weight loss.

hexane, and chloroform, respectively. The chloroform solution was concentrated and the product re-precipitated in methanol to obtain the resulting copolymers. Table 1 summarized the polymerization results and thermal properties of the copolymers.

The polymers can be readily dissolved in common organic solvents, such as chloroform, tetrahydrofuran (THF), chlorobenzene, and 1,2-dichlorobenzene at room temperature or with a slight heating. The molecular weights and polydispersity indices (PDIs) of the copolymers were determined by gel permeation chromatography (GPC) analysis with a polystyrene standard calibration and THF as an eluent. The four copolymers showed relatively big difference in the molecular weights. **PBDT-AT** gave a high weight-average molecular weight (M_w) of 103.2 kDa with a large PDI of 5.76 (Table 1). However, **PBDT-TT** showed a low M_w of 6.2 kDa with a small PDI of 1.38 (Table 1). It can be seen that the copolymers (**PBDT-TT** and **PDTS-TT**) with TT as the conjugated bridge have lower molecular weights than those of the copolymers (**PBDT-AT** and **PDTS-AT**) with AT as the conjugated bridge, which could result from the poorer solubility of the former. One possible reason could be ascribed to the absence of alkyl groups in the TT bridge. High molecular weight is desirable because it will help to improve the film-forming ability and photovoltaic performance. It has previously been demonstrated in the cases of poly(3-hexylthiophene) and other D–A polymers that molecular weight has a significant impact on optoelectronic properties.[4a]

Thermal properties of the polymers were determined by thermogravimetric analysis (TGA) under nitrogen atmosphere at a heating rate of 20 °C min^{-1}. The four polymers had good thermal stability with onset decomposition temperatures corresponding to 5% weight loss (T_d) at above 290 °C, as shown in Table 1. Obviously, the thermal stability of the polymers is adequate for the applications in PSCs and other optoelectronic devices.

Optical Properties

Figure 2 shows absorption spectra of the four polymers in dilute chloroform solution and as thin solid films. The detailed absorption data including the absorption maximum wavelength (λ_{max}) in both solution and films, the absorption edge (onset wavelength of the absorption peak, λ_{edge}) of the polymer films, and optical bandgaps (E_g^{opt}) are summarized in Table 2.

Except **PDTS-TT**, the absorption spectra of other three polymers recorded from dilute chloroform solutions feature two absorption bands in the range of 300–800 nm [Fig. 2(a)]: the first one located at 330–390 nm can be assigned to

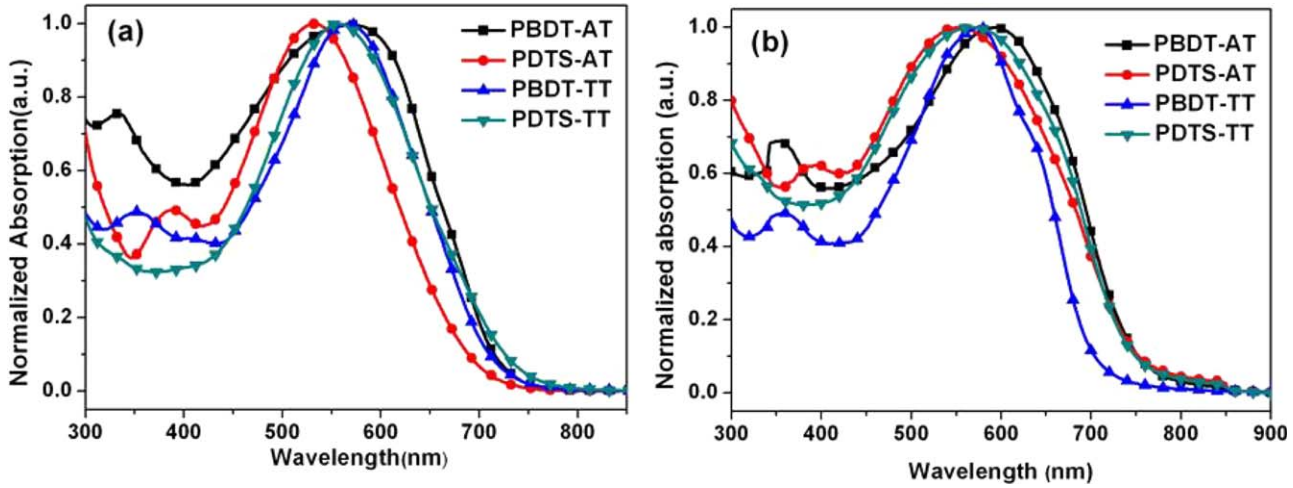

FIGURE 2 Absorption spectra of the four D-π-A copolymers in dilute chloroform solution (**a**) and solid film on a quartz plate (**b**). [Color figure can be viewed in the online issue, which is available at wileyonlinelibrary.com.]

TABLE 2 Optical and Electrochemical Properties of the Four Copolymers

Copolymer	Solution λ_{smax} (nm)	Film λ_{fmax} (nm)	λ_{edge} (nm)[a]	E_g^{opt} (eV)[b]	E_{HOMO} (eV)	E_{LUMO} (eV)
PBDT-AT	330, 568	354, 594	740	1.68	−5.30	−3.78
PDTS-AT	388, 534	392, 552	748	1.66	−5.31	−3.57
PBDT-TT	350, 568	356, 576	697	1.78	−5.14	−3.39
PDTS-TT	556	566	739	1.68	−5.18	−3.59

[a] Absorption edge of the thin films.

[b] Estimated from the absorption edge: $E_g^{opt} = 1{,}240/\lambda_{edge}$.

localized π–π^* transition, and the second broader band from 400 to 750 nm in the long wavelength region corresponds to ICT between donor and acceptor units. For the four polymers the difference in position and shape of the absorptions are mainly due to different structures of the π-bridges and donors in the polymers. Compared with **PDTS-AT**, the absorption spectrum of **PBDT-AT** is broader and the λ_{max} of ICT peak is red-shifted remarkably (568 vs. 534 nm), which indicates that different electron donating strength of the donor units (BDT vs. DTS) had a great influence on the absorption. Similar phenomenon can be found to compare **PBDT-TT** with **PDTS-TT**. Additionally, **PDTS-TT** displays a red-shifted λ_{max} of ICT peak relative to **PDTS-AT**, revealing the effect of the different π-bridges on the optical properties of the D-π-A copolymers. In contrast, **PBDT-TT** exhibits a blue-shifted λ_{max} compared with **PBDT-AT**, which mainly results from the low polymerization degree of the former with the significantly low molecular weight. The absorption spectra of the polymer films are broader and obviously red-shifted in comparison with those of their solutions [Fig. 2(b)], indicating intermolecular interactions existing in the solid state. In a word, **PBDT-AT** possesses broader and red-shifted absorption spectrum compared with the other three polymers, indicating a higher J_{sc} could be obtained in solar cells. The absorption edges (λ_{edge}) for solid films of the four polymers varied from 697 to 748 nm, corresponding to

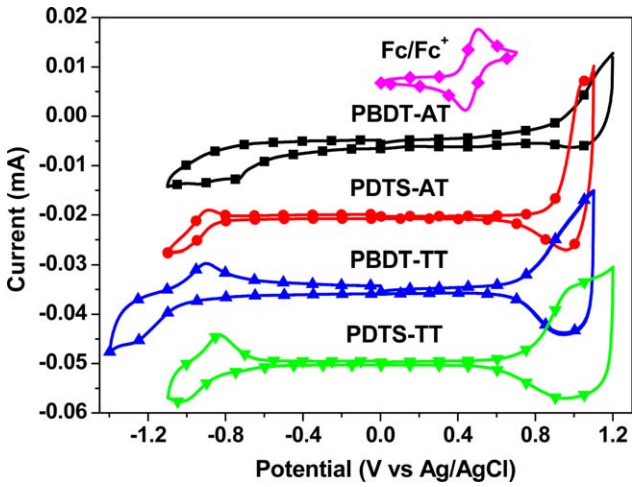

FIGURE 3 Cyclic voltammograms of the polymer films on platinum electrode in acetonitrile solution containing 0.1 mol L^{-1} Bu_4NPF_6 at a scan rate of 0.1 V s^{-1}. The cyclic voltammogram of ferrocene was also put in the figure for the potential calibration. [Color figure can be viewed in the online issue, which is available at wileyonlinelibrary.com.]

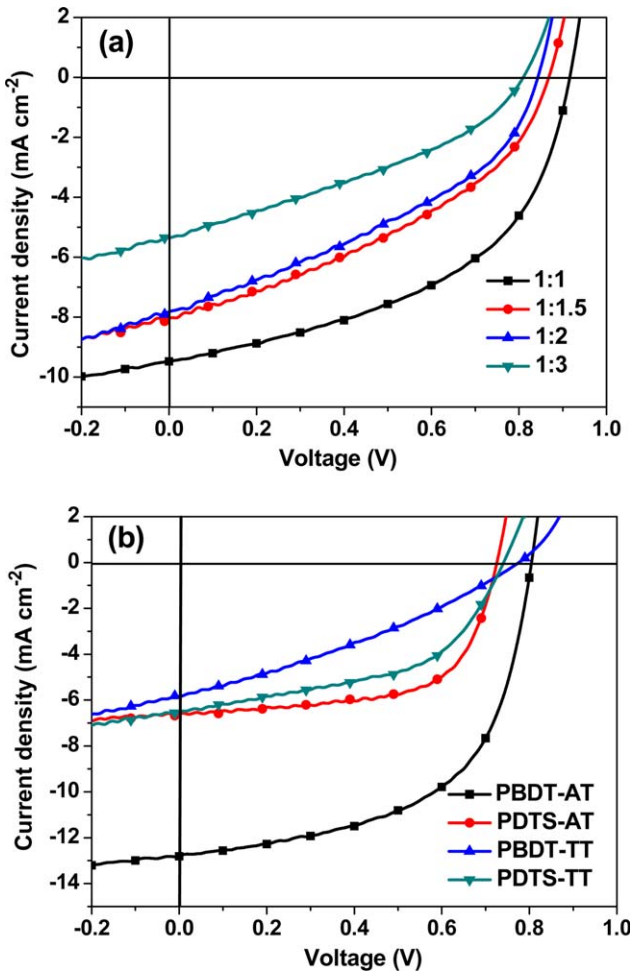

FIGURE 4 (**a**) *J–V* curves of the PSCs based on **PBDT-AT** with different donor/acceptor ratios; (**b**) *J–V* curves of the optimized PSCs based on the four polymers with a certain amount of DIO additive and treatment of methanol. [Color figure can be viewed in the online issue, which is available at wileyonlinelibrary.com.]

TABLE 3 Photovoltaic Properties of the PSCs Based on the Copolymers:$PC_{70}BM$ with Different Fabrication Conditions, Under the Illumination of AM1.5, 100 mW cm^{-2}

Active Layer	DIO	MeOH	V_{oc} (V)	J_{sc} (mA cm^{-2})	FF (%)	PCE (%)
PBDT-AT:$PC_{70}BM$ = 1:1	−	−	0.92	9.47	49.2	4.27
PBDT-AT:$PC_{70}BM$ = 1:1.5	−	−	0.87	8.02	39.0	2.72
PBDT-AT:$PC_{70}BM$ = 1:2	−	−	0.84	7.80	37.8	2.48
PBDT-AT:$PC_{70}BM$ = 1:3	−	−	0.81	5.36	34.7	1.51
PBDT-AT:$PC_{70}BM$ = 1:1	3%	−	0.85	10.28	55.0	4.81
PBDT-AT:$PC_{70}BM$ = 1:1	5%	−	0.82	12.72	52.4	5.46
PBDT-AT:$PC_{70}BM$ = 1:1	7%	−	0.82	11.37	53.9	4.99
PBDT-AT:$PC_{70}BM$ = 1:1	5%	+	0.81	12.81	57.3	5.91
PDTS-AT:$PC_{70}BM$ = 1:3	−	−	0.75	4.66	54.0	1.89
PDTS-AT:$PC_{70}BM$ = 1:3	3%	−	0.71	7.68	48.1	2.62
PDTS-AT:$PC_{70}BM$ = 1:3	3%	+	0.73	6.61	63.3	3.06
PBDT-TT:$PC_{70}BM$ = 1:1.5	−	−	0.78	2.81	26.5	0.58
PBDT-TT:$PC_{70}BM$ = 1:1.5	3%	−	0.78	3.42	30.6	0.82
PBDT-TT:$PC_{70}BM$ = 1:1.5	3%	+	0.78	5.85	31.7	1.45
PDTS-TT:$PC_{70}BM$ = 1:2	−	−	0.71	6.37	43.6	1.97
PDTS-TT:$PC_{70}BM$ = 1:2	5%	−	0.73	6.47	50.3	2.38
PDTS-TT:$PC_{70}BM$ = 1:2	5%	+	0.74	6.47	51.2	2.45

optical bandgaps (E_g^{opt}) from 1.78 to 1.66 eV, as shown in Table 2. It should be noted that BDT-based polymer **PBDT-AT** displayed lower bandgap (1.68 eV) than that of its analogue without a π-bridge (1.78 eV).[9]

Electrochemical Properties

The HOMO and LUMO energy levels of conjugated polymers are crucial for the application as photovoltaic materials in PSCs, and they can be measured from the onset oxidation and reduction potentials ($E_{ox/red}$) in the cyclic voltammograms of the polymers.[12] Figure 3 shows the cyclic voltammograms of the four polymer films on Pt electrode in a 0.1 mol L^{-1} Bu_4NPF_6 acetonitrile solution. The results of the electrochemical properties are also summarized in Table 2. The cyclic voltammograms were recorded by using a Ag/AgCl reference electrode, which was calibrated against the redox potential of ferrocene/ferrocenium couple, whose energy level was assumed to be 4.80 eV below the vacuum level.[13] Fc/Fc^+ was measured to be 0.40 V versus Ag/AgCl, thus $E_{HOMO/LUMO} = -e(E_{ox/red} + 4.40)$ (eV), where $E_{ox/red}$ is the onset oxidation/reduction potential (vs. Ag/AgCl) of the polymers.

The $E_{ox/red}$ values of **PBDT-AT, PDTS-AT, PBDT-TT**, and **PDTS-TT** are 0.90/−0.65, 0.91/−0.83, 0.74/−1.01, and 0.78/−0.81 V versus Ag/AgCl, respectively. Based on the $E_{ox/red}$ values of the polymers, the $E_{HOMO/LUMO}$ values of **PBDT-AT, PDTS-AT, PBDT-TT**, and **PDTS-TT** were calculated to be −5.30/−3.75, −5.31/−3.57, −5.14/−3.39, and −5.18/−3.59 eV, respectively, which are listed in Table 2. The HOMO energy levels of **PBDT-AT** and **PDTS-AT** are very close and the same results can be found from **PBDT-TT** and **PDTS-TT**. However, there is a considerable difference in the HOMO energy levels for **PBDT-AT** and **PDTS-AT** compared with **PBDT-TT** and **PDTS-TT**. These phenomena indicate that the different π-bridges have more significant effect on the HOMO energy levels than that of the different donor units in the D-π-A copolymers. In addition, the lower-lying HOMO energy levels of **PBDT-AT** and **PDTS-AT** compared with those of **PBDT-TT** and **PDTS-TT** is expected to give an increase in V_{oc} of PSCs. On the other hand, the LUMO energy levels of the four polymers vary from −3.39 to −3.75 eV, implying both the different donor units and π-bridges have influence on the LUMO energy levels. It is well known that an appropriate LUMO/HOMO energy level offset between a polymer donor and a fullerene acceptor (e.g., $PC_{70}BM$) should be larger than 0.3–0.5 eV for efficient exciton dissociation on the donor/acceptor interfaces. The HOMO and LUMO energy levels of $PC_{70}BM$ are −5.87 and −3.91 eV, respectively.[14] Obviously, the LUMO and HOMO energy levels of the polymers are suitable for the application as donor materials with $PC_{70}BM$ as acceptor in the BHJ PSCs. In addition, the HOMO energy levels of the polymers are lower than −5.20 eV which is desirable for ambient stability to oxidation.[15]

Photovoltaic Properties

To investigate the effect of donor unit and π-conjugated bridge on the photovoltaic properties of the D-π-A copolymers, BHJ PSCs with a configuration of ITO/PEDOT:PSS/polymer:$PC_{70}BM$/Ca/Al were fabricated. Figure 4 shows the current density–voltage (*J-V*) curves of the PSCs under the illumination of AM1.5G, 100 mW cm^{-2}. The corresponding open-circuit voltage (V_{oc}), short-circuit current density (J_{sc}), fill factor (FF), and PCE of the devices are summarized in Table 3.

First, the blend ratio of the polymer donor and $PC_{70}BM$ acceptor was optimized. For example, when the mixing ratio of **PBDT-AT** and $PC_{70}BM$ changed from 1:1 to 1:3, the PCE of the device continuously decreased from 4.27% to 1.51% [Fig. 4(a); Table 3], due to the decrease of both V_{oc} and FF of the PSCs. It was observed that an increase in the $PC_{70}BM$ content resulted in a slight decrease in the V_{oc}, which has been observed for other donor polymers.[16] The reduction in the V_{oc} correlated with the decrease in the energy of the charge transfer (CT) states with increasing $PC_{70}BM$ concentrations.[16d] Therefore, the optimal blend ratio for this polymer was determined to be around 1:1. The blend ratio of the other three polymers was also optimized. It was found that the different polymers have their own optimal blend ratio and the determined optimal blend ratios are 1:3, 1:1.5, and 1:2, for **PDTS-AT, PBDT-TT**, and **PDTS-TT**, respectively. Next, the effect of a processing additive, such as 1,8-diiodooctane (DIO), upon the photovoltaic properties of the PSCs was explored, the results are shown in Table 3. We take **PBDT-AT** as an example, when DIO was added as the processing additive, the J_{sc} and FF values can be improved significantly, resulting in remarkably improvement of PCEs even though the V_{oc} values dropped in some extend. The decrease of the V_{oc} values could result from increased charge carrier recombination due to the changed interpenetrating network by DIO additive treatment. Moreover, the concentration of the DIO additive was optimized. For the **PBDT-AT**–based PSCs, the PCE was improved up to 5.46% with 5 vol % DIO additive, with a V_{oc} of 0.82 V, a J_{sc} of 12.72 mA cm^{-2} and a FF of 52.4%. For other polymers, the photovoltaic performance was also improved with a certain amount of DIO additive. The PCEs of the optimized PSCs based on **PDTS-AT, PBDT-TT**, and **PDTS-TT** were 2.62%, 0.82%, and 2.38%, respectively (see Table 3).

Inspired by recent work on post solvent treatment,[17] we tried to employ a polar solvent methanol to further optimize the photovoltaic performance of PSCs with the following procedure: (i) spin-coating the active layer and dried in inert atmosphere; (ii) methanol was added on top of the active layer and left for a very short time (such as 10 sec); (iii) methanol was removed by spin-coating at high speed (such as 2500 rpm); (iv) the metal cathode (Ca and Al) was evaporated on the active layer. The results are shown in Figure 4(b) and Table 3. It can be seen that after the solvent treatment the photovoltaic performance of all the copolymers was enhanced. For **PBDT-AT**, the PCE was further improved up to 5.91% with an increased J_{sc} from 12.72 to 12.81 mA cm^{-2}, and a FF from 52.4% to 57.3%. For **PDTS-AT**, the PCE increased from 2.62% to 3.06%, with a V_{oc} from 0.71 to 0.73 V and a largely increased FF from 48.1% to 63.3%. For **PBDT-TT**, the PCE achieved 1.45%, mainly due to an obviously improved J_{sc} from 3.42 to 5.85 mA cm^{-2}. As for **PDTS-TT**, there was a slightly increased PCE up to 2.45%. Moreover, the PCE of 5.91% for **PBDT-AT** is significantly higher than that of the analogy polymer (2.18%)[9] without π-bridge, indicating the importance of a π-bridge to achieve high performance D-π-A copolymers. The improved efficiency may originate from enhanced charge transport, or improved efficiency of charge carrier collection, which can all result from the creation of an optimal morphology under the treatment of DIO additive and methanol. The morphology will be discussed in detail below.

V_{oc} value of the PSC based on **PBDT-AT** is higher than those of the PSCs based on **PBDT-TT** and **PDTS-TT**, which can be readily understood from the lower-lying HOMO energy level of **PBDT-AT** (Table 2). But, the relatively lower V_{oc} of the PSC based on **PDTS-AT** with a low-lying HOMO energy level could be due to poorer morphology of its active layer or other reasons.[18] The highest J_{sc} values of PSCs based on these polymers increased from 5.85 mA cm^{-2} for **PBDT-TT** to 6.47 mA cm^{-2} for **PDTS-TT** to 7.68 mA cm^{-2} for **PDTS-AT** to 12.81 mA cm^{-2} for **PBDT-AT**, which are consistent with the broadened absorption of the corresponding polymers. It should be noted that the J_{sc} based on **PDTS-TT** is obvious lower than that of **PBDT-AT** even though they have the similar broad spectra, which should be ascribed to the different molecular weight of the polymers. The lower molecular weight PDTS-TT showed lower J_{sc} and the higher molecular weight PBDT-AT demonstrated higher J_{sc} (see Fig. 2; Tables 1 and 2).

Figure 5 displays the external quantum efficiency (EQE) curves of the PSC. The PSCs based on these polymers exhibit broad EQE responses ranging from 300 to 750 nm with maximum EQE values of 67% at 555 nm, 44% at 470 nm, 42% at 500 nm, and 44% at 494 nm for **PBDT-AT, PDTS-AT, PBDT-TT**, and **PDTS-TT**, respectively. Compared with the absorption spectra of polymer films [Fig. 2(b)], the significantly broadened EQE responses in the visible region can be attributed to both the intrinsic absorption of the polymers and $PC_{70}BM$. The EQE results are consistent with the J_{sc} values of the corresponding PSCs, and PBDT-AT showed the highest EQE values corresponding to the highest J_{sc} value of the PSC based on PBDT-AT.

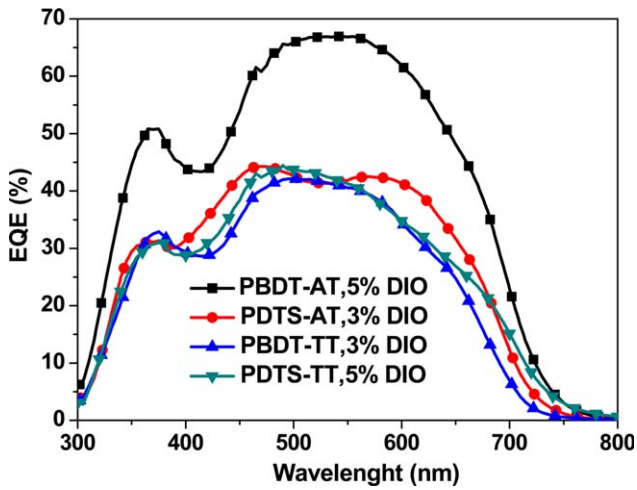

FIGURE 5 Typical EQE curves of solar cells of the four polymers with methanol treatment. [Color figure can be viewed in the online issue, which is available at wileyonlinelibrary.com.]

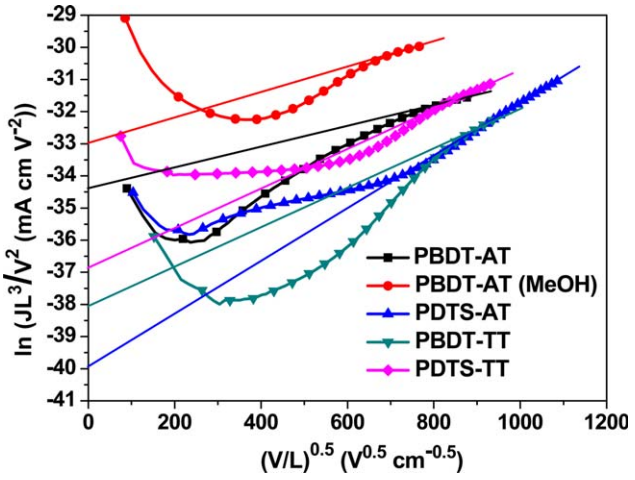

FIGURE 6 Plots of $\ln(JL^3\ V^{-2})$ versus $(V^{0.5}\ L^{-0.5})$ of the device ITO/PEDOT:PSS/blended film/Au for the measurement of hole mobility. [Color figure can be viewed in the online issue, which is available at wileyonlinelibrary.com.]

To investigate crystalline behavior of the polymers, we made the X-ray diffraction (XRD) analysis of the four polymer films, as shown in Figure S1 in Supporting Information. The XRD patterns of the four films in Supporting Information Figure S1 exhibit no obvious diffraction peaks, which mean these four polymer films were amorphous. This could be a reason for relatively lower FF for the PSCs based on these polymers.

Hole mobility is a very important parameter for conjugated polymer donor photovoltaic materials. Here, the hole mobility of the polymer/$PC_{70}BM$ blend film with the optimal D/A ratio (w/w) was measured by the space-charge limited current (SCLC) method on a hole-only device with a structure of ITO/PEDOT:PSS/polymer:$PC_{70}BM$/Au and estimated through the Mott–Gurney equation.[19] Figure 6 shows the $\ln(JL^3/V^2)$ versus $(V/L)^{0.5}$ plot of the blend films. The hole mobilities of the polymers calculated are 4.52×10^{-3}, 1.84×10^{-5}, 1.23×10^{-4}, and 4.09×10^{-4} $cm^2\ V^{-1}\ s^{-1}$ for **PBDT-AT, PDTS-AT, PBDT-TT**, and **PDTS-TT**, respectively. It should be noted that the hole mobility of polymer:$PC_{70}BM$ blend was enhanced dramatically after treatment with methanol. For example, the hole mobility of **PBDT-AT**-based blend treated with methanol was increased by three times, from 4.52×10^{-3} to 1.83×10^{-2} $cm^2\ V^{-1}\ s^{-1}$. The improved hole mobility could be ascribed to the better nanoscale morphology of the active layer after methanol treatment. The higher hole mobility could contribute in part to the higher J_{sc} and FF values of the devices with methanol treatment (see Table 3).[17e,f] The higher hole mobility of the **PBDT-AT–**based blend film could be related to its higher molecular

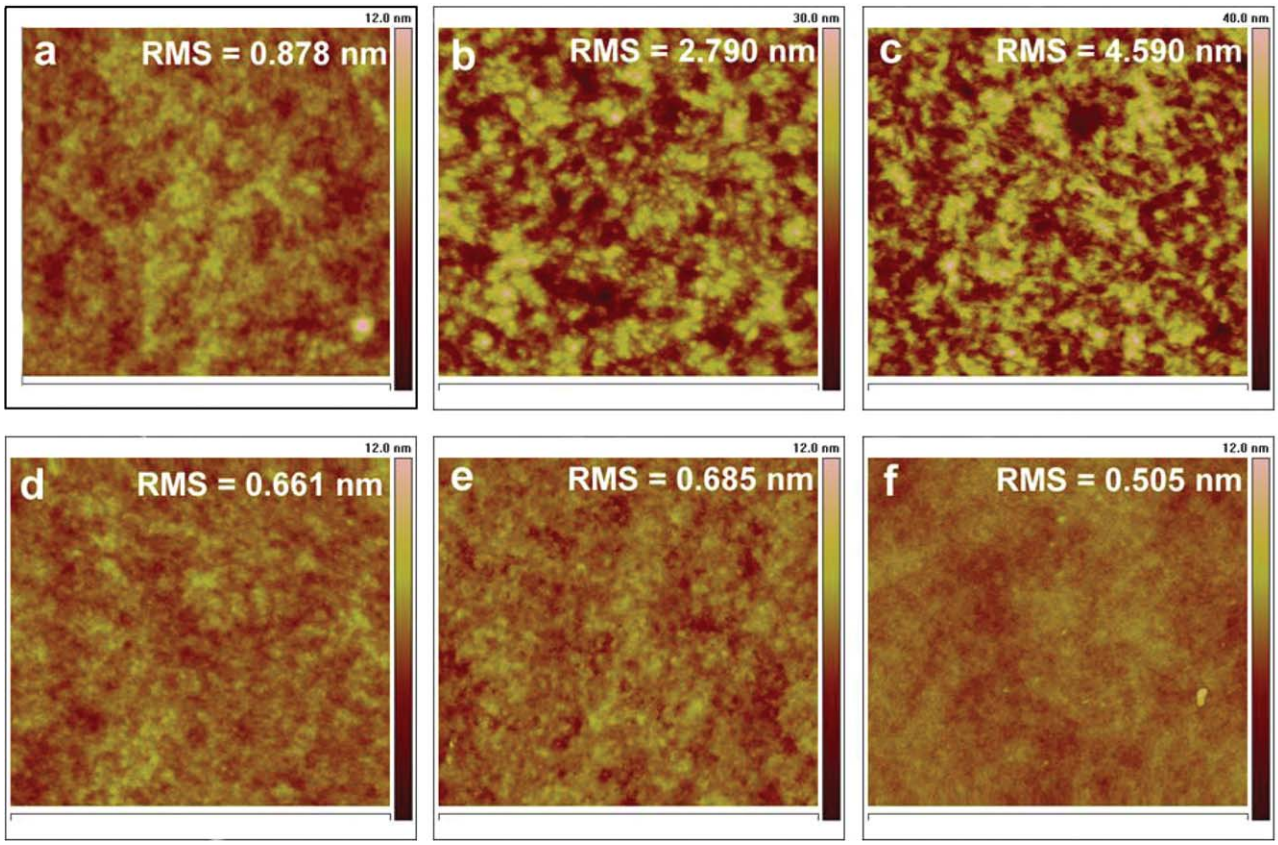

FIGURE 7 AFM height images of (**a**) **PBDT-AT**:$PC_{70}BM$ (1:1), (**b**) **PBDT-AT**:$PC_{70}BM$ (1:1, 5 vol % DIO), (**c**) **PBDT-AT**:$PC_{70}BM$ (1:1, 5 vol % DIO, treated with methanol), (**d**) **PDTS-AT**:$PC_{70}BM$ (1:3), (**e**) **PDTS-TT**:$PC_{70}BM$ (1:1.5), and (**f**) **PDTS-TT**:$PC_{70}BM$ (1:2) blend films. The imaging size is 5 μm × 5 μm for each panel.

weight (see Table 1).[4a,20] While for the other three polymers with relatively lower molecular weight, the hole mobilities of the polymers with TT as the π-bridge (**PBDT-TT** and **PDTS-TT**) are one order of magnitude higher than that of the polymer with AT as the π-bridge (**PDTS-AT**), which indicates that TT π-bridge in the D-π-A copolymers is beneficial to higher hole mobility of the polymers because of its planar and larger molecular plane.[6f]

To explore the effect of the morphology of active layers on the photovoltaic performance of the four D-π-A copolymers, we observed the surface morphologies of the blend films using atomic force microscopy (AFM). Figure 7 gives the AFM height images of the active layer surfaces. It can be seen that the surface of the active layers of polymer:$PC_{70}BM$ without DIO additive is very smooth, with a root-mean-square (RMS) of 0.878, 0.661, 0.685, and 0.505 nm for **PBDT-AT, PDTS-AT, PBDT-TT**, and **PDTS-TT**, respectively. The active layer of **PBDT-AT** showed a relative rougher surface compared with the other three polymers, which suggests that relative larger phase separation is more favorable for charge transport. After adding the DIO additive (e.g., 5 vol % for **PBDT-AT** blend film), the surface roughness of the active layer based on **PBDT-AT** increased to a RMS of 2.790 nm [see Fig. 7(b)]. Moreover, after methanol treatment the surface roughness of the blend film further increased to a RMS of 4.59 nm, and the surface demonstrated a more uniform interpenetrating network of **PBDT-AT** and $PC_{70}BM$ [see Fig. 7(c)]. The long-range interpenetrating network in the active layer of PBDT-AT/$PC_{70}BM$ after methanol treatment should be beneficial to the exciton dissociation and charge carriers transport. The appropriate surface roughness at about 4–5 nm and the improved interpenetrating network of the polymer/$PC_{70}BM$ blend should be responsible for the superior photovoltaic performance of the **PBDT-AT**-based PSCs with methanol treatment (see Table 3).

CONCLUSIONS

In summary, four D-π-A type copolymers **PBDT-AT, PDTS-AT, PBDT-TT**, and **PDTS-TT**, based on the same BDD acceptor unit with different donor units and π-bridges, were designed and synthesized via a Pd-catalyzed Stille-coupling method. Two kinds of donor units (BDT and DTS) and π-bridges (AT and TT) were employed to fully investigate the effect of the different donor units and π-bridges upon the optical and electrochemical properties, hole mobilities, and photovoltaic performance of the copolymers. These D-π-A copolymers possessed broad absorption (ranging from 300 to 800 nm) and lower energy bandgaps (from 1.66 to 1.78 eV). The polymers with BDT as the donor unit showed broader and red-shifted absorption spectra compared with the counterparts with DTS as the donor unit. And the polymers with TT π-bridge gave red-shifted absorption spectra than that of the polymers with AT π-bridge although the molecular weight of the polymers with TT π-bridge is lower. The results of electrochemical measurements revealed that the π-bridges have more obvious effect on the HOMO energy levels than that of the donor units in the D-π-A polymers, and the polymers with TT π-bridge show up-shifted HOMO energy level than that of the polymers with AT π-bridge. PCE of the PSCs based on **PBDT-AT** with methanol treatment reached 5.91%, which is greatly improved in comparison with the corresponding polymer without the AT π-bridge. The effect of methanol treatment on the enhancement of photovoltaic performance is revealed to originate from the increased carrier transport and the formation of better nanoscaled interpenetrating network. This work provides a good example for tuning absorption properties, energy levels, charge transport and photovoltaic properties of the D-π-A copolymers by appropriate combination of the donor units and π-bridges. Most importantly, this study clearly proves that BDD is a promising acceptor unit to construct D-A copolymers for high-performance photovoltaic materials.

EXPERIMENTAL

Measurements and Characterization

^1H NMR spectra and ^{13}C NMR spectra were measured on a Bruker DMX-400 spectrometer with $CDCl_3$ as the solvent and trimethylsilane as the internal reference. UV–visible (UV–vis) absorption spectra were measured on a Hitachi U-3010 UV–vis spectrophotometer. Mass spectra (MS) were recorded on a Shimadzu spectrometer and MALDI-TOF-MS spectra were determined on a Bruker BIFLEX III mass spectrometer. TGA was conducted on a Perkin–Elmer TGA-7 thermogravimetric analyzer at a heating rate of 20 °C min^{-1} and under a nitrogen flow rate of 100 mL min^{-1}. Molecular weights of the polymers were measured by GPC method on Waters 515-2410 with polystyrenes as standard and THF as an eluent. The electrochemical cyclic voltammetry was performed on a Zahner IM6e Electrochemical Workstation, with a Pt disk coated with the polymer film, Pt wire, and Ag/AgCl electrode as the working electrode, counter electrode, and reference electrode, respectively, in a 0.1 mol L^{-1} tetrabutylammonium hexafluorophosphate (Bu_4NPF_6) acetonitrile solution. The morphology of blend films was measured using an AFM (Digital Instrument Multimode Nanoscope IIIA) with the tapping mode.

PSC Device Fabrication and Characterization

The PSC devices were fabricated with a structure of ITO/PEDOT:PSS/polymer:PCBM/Ca/Al. The patterned ITO glass was precleaned in an ultrasonic bath of acetone and isopropanol and treated in an ultraviolet-ozone chamber (Jelight Co.) for 30 min. A thin layer of PEDOT:PSS [poly(3,4-ethylenedioxythiophene):poly(styrenesulfonate)] was spin-cast on precleaned ITO-coated glass from a PEDOT:PSS aqueous solution (Baytron P VP AI 4083 from H. C. Starck) at 3000 rpm and dried subsequently at 150 °C for 30 min in air, then the device was transferred to a glovebox, where a blend solution of the polymer and $PC_{70}BM$ with the polymer concentration of 10 mg mL^{-1} was spin-coated onto the PEDOT:PSS layer. Finally, a Ca/Al metal top electrode was deposited in vacuum onto the active layer at a pressure of about 5×10^{-5} Pa. The active area of the device was about

4 mm^2. The current density–voltage (J–V) characteristics were measured on a computer-controlled Keithley 236 Source–Measure Unit. A xenon lamp (150 W) coupled with AM 1.5 solar spectrum filter was used as the light source, and the optical power at the sample was 100 mW cm^{-2}. EQE spectrum was measured by a Stanford Research Systems model SR830 DSP lock-in amplifier coupled with WDG3 monochromator and a 150 W Xenon lamp. The hole mobility was calculated by fitting the dark J–V curves for the hole-only devices with SCLC model at low voltages, in which the current density is given by $J = 9\varepsilon_0\varepsilon_r\mu V^2/8L^3\exp[0.891\gamma(V/L)^{0.5}]$, where $\varepsilon_0\varepsilon_r$ represents the permittivity of the material, μ is the mobility, γ is the field activation factor, and L the thickness of the active layer. The applied bias voltage is corrected for the built-in potential so that $V = V_{applied} - V_{bi}$.

Synthesis of Monomers and Polymers

3,4-Thiophenedicarboxylic acid, 3-hexylthiophene, oxalyl chloride, NBS, 1-bromo-2-ethylhexane, 1-bromo-2-hexyldecane, TT, anhydrous $AlCl_3$, and $Pd(PPh_3)_4$ were purchased from J&K Chemical or Alfa Aesar. Toluene was distilled from sodium benzophenone under nitrogen before use. All other reagents and solvents used in this work were commercially purchased and used without further purification. All chromatographic separations were carried out on silica gel (200–300 mesh). Compounds 2-(2-ethylhexyl)thiophene,[21] 2-(2-hexyldecyl)thiophene,[21] 2-(tributylstannyl)thieno[3,2-*b*]thiophene,[21] tributyl(4-hexylthiophen-2-yl)stannane,[21] monomers **M3**,[7b] **M4**,[7b] and **M5**[11] were synthesized according to the procedure reported in the literatures. The detailed synthetic processes of other compounds are as follows.

2,5-Dibromothiophene-3,4-dicarboxylic acid (**1**). Thiophene-3,4-dicarboxylic acid (5.00 g, 29.1 mmol) and glacial acetic acid (50.0 mL) were added to a 250 mL flask with a stirring bar. Bromine (9.00 mL, 174 mmol) was added dropwise. The mixture was stirred overnight. Aqueous sodium bisulfate solution was added until the reddish color disappeared. The mixture was filtered and washed with 50 mL water, and compound **1** was afforded as a gray solid (9.00 g, yield: 75%). MS *m/z*: [M^+] calculated for $C_6H_2Br_2O_4S$, 329.8; found, 330.

2,5-Dibromothiophene-3,4-dicarboxylic acid chloride (**2**). Oxalyl chloride (5.30 mL, 60.5 mmol) was slowly added to compound **1** (5.00 g, 15.2 mmol) and DMF (one drop) in dry dichloromethane (100 mL). The mixture was stirred overnight under room temperature. The volatiles were removed in vacuum, and a brown product as compound **2** was directly used in the next step without further purification.

5,7-Dibromo-2-(2-ethylhexyl)benzo[1,2-*b*:4,5-*c*']dithiophene-4,8-dione (**3**). To a stirred solution of compound **3** (3.65 g, 10.0 mmol) and 2-(2-ethylhexyl)thiophene (2.16 g, 11.0 mmol) in dry dichloromethane, anhydrous $AlCl_3$ (3.00 g, 22.5 mmol) was added in small portions at 0 °C. The mixture was stirred at 0 °C for 1 h, and then at room temperature for additional 5 h. The reaction mixture was poured into a mixture of ice water and 1 M hydrochloric acid and extracted with dichloromethane. The organic layer was washed with brine and dried over anhydrous $MgSO_4$, and the solvent was removed under vacuum. The crude product was purified through the silica gel column with petroleum ether/dichloromethane (2:1 by volume) as eluent to give compound **3** as a yellow solid (0.63 g, yield 12.9%). ^{1}H NMR (400 MHz, $CDCl_3$): δ (ppm) 7.21 (s, 1H), 2.78–2.76 (d, 2H, J = 6.68 Hz), 1.60–1.54 (m, 1H), 1.34–1.19 (m, 8H), 0.87–0.82 (m, 6H). MALDI-TOF-MS *m/z*: [M^+] calculated for $C_{18}H_{18}Br_2O_2S_2$, 491.9; found, 491.7.

2-(2-Ethylhexyl)-5,7-bis(4-hexylthiophen-2-yl)benzo[1,2-*b*:4,5-*c*']dithiophene-4,8-dione (**4a**). A solution of compound **3** (1.57 g, 3.20 mmol) and 4-hexyl-2-(tributylstannyl)thiophene (4.16 g, 8.00 mmol) in freshly distilled toluene (35 mL) was degassed. Under an argon atmosphere the $Pd(PPh_3)_4$ (220 mg, 0.19 mmol) was added. And then the mixture was heated and refluxed for 24 h, toluene was removed by vacuum distillation. The crude product was purified through the silica gel column with petroleum ether/dichloromethane (4:1 by volume) to give compound **4a** as a wine red solid (1.45 g, yield 68%). ^{1}H NMR (400 MHz, $CDCl_3$): δ (ppm) 7.73–7.71 (d, 2H, J = 8.80 Hz), 7.33 (s, 1H), 7.14 (s, 2H), 2.83 (d, 1H, J = 6.44 Hz), 2.65 (t, 4H, J = 7.08 Hz), 1.66–1.62 (m, 5H), 1.36–1.29 (m, 20H), 0.94–0.88 (m, 12H). MALDI-TOF-MS *m/z*: [M^+] calculated for $C_{38}H_{48}O_2S_4$, 666.3; found, 666.7.

2-(2-Ethylhexyl)-5,7-bis(thieno[3,2-*b*]thiophen-2-yl)benzo[1,2-*b*:4,5-*c*']dithiophene-4,8-dione (**4b**). This compound was obtained as a red solid (yield 57%) from the reaction of compound **3** and 2-(tributylstannyl)thieno[3,2-b]thiophene according to the similar procedure described for the synthesis of compound **4a**. ^{1}H NMR (400 MHz, $CDCl_3$): δ (ppm) 8.20 (s, 1H), 8.17 (s, 1H), 7.50–7.48 (m, 2H), 7.28 (s, 1H), 7.25–7.24 (m, 2H), 2.83–2.78 (m, 2H), 1.65–1.62 (m, 1H), 1.38–1.29 (m, 8H), 0.94–0.87 (m, 6H). ^{13}C NMR (100 MHz, $CDCl_3$, δ/ppm): 175.84, 174.21, 155.59, 145.46, 144.38, 144.26, 144.12, 142.50, 139.53, 139.44, 134.40, 134.30, 130.49, 130.10, 127.36, 124.48, 123.60, 123.47, 119.44, 41.39, 34.81, 32.37, 28.81, 25.57, 22.93, 14.09, 10.79. MALDI-TOF-MS *m/z*: [M^+] calculated for $C_{30}H_{24}O_2S_6$, 609.0; found, 609.2.

5,7-Bis(5-bromo-4-hexylthiophen-2-yl)-2-(2-ethylhexyl)-benzo[1,2-*b*:4,5-*c*']dithiophene-4,8-dione (**M1**). NBS (0.65 g, 3.60 mmol) in DMF (15 mL) was added dropwise to a solution of compound **4a** (1.20 g, 1.80 mmol) in DMF (35 mL), which was cooled in an ice bath. After complete addition, the reaction mixture was allowed to warm to room temperature and stirred for overnight. The reaction mixture was poured into water and extracted with chloroform. The organic layers were combined, washed with brine, and dried with anhydrous $MgSO_4$. Further purification was performed through silica gel chromatography using petroleum ether/dichloromethane (6:1 by volume) to give monomer **M1** (1.27 g, yield 86%) as a deep red solid. ^{1}H NMR (400 MHz, $CDCl_3$): δ (ppm) 7.51 (s, 1H),

7.50 (s, 1H), 7.33 (s, 1H), 2.83 (d, 2H, J = 6.48 Hz), 2.60 (t, 4H, J = 6.81 Hz), 1.63–1.58 (m, 5H), 1.34–1.29 (m, 20H), 0.91–0.88 (m, 12H). ^{13}C NMR (100 MHz, $CDCl_3$, δ/ppm): 175.77, 174.19, 155.77, 145.13, 144.06, 143.19, 142.81, 142.43, 132.21, 132.17, 132.50, 129.45, 129.11, 124.45, 116.49, 41.38, 34.83, 32.39, 31.62, 29.72, 29.50, 29.00, 28.82, 25.55, 22.93, 22.62, 14.09, 10.79. MALDI-TOF-MS *m/z*: [M^+] calculated for $C_{38}H_{48}Br_2O_2S_4$, 824.1; found, 824.6.

5,7-Bis(5-bromothieno[3,2-*b*]thiophen-2-yl)-2-(2-ethylhexyl)benzo[1,2-*b*:4,5-*c*']dithiophene-4,8-dione (**M2**). This compound was obtained as a dark red solid (yield 85%) from the reaction of compound **4b** and NBS according to the similar procedure described for the synthesis of monomer **M1**. ^{1}H NMR (400 MHz, $CDCl_3$): δ (ppm) 8.04 (s, 1H), 8.00 (s, 1H), 7.23 (s, 2H), 7.22 (s, 1H), 4.15–4.09 (m, 1H), 2.77–2.76 (d, 2H, J = 6.80 Hz), 1.56–1.23 (m, 8H), 0.92–0.88 (m, 6H). ^{13}C NMR (100 MHz, $CDCl_3$, δ/ppm): 175.49, 173.85, 155.71, 145.10, 143.86, 143.62, 143.33, 141.76, 141.71, 139.56, 139.48, 133.80, 133.72, 130.48, 130.11, 124.31, 122.87, 122.75, 122.07, 177.16, 41.31, 34.76, 32.36, 28.78, 25.52, 22.97, 14.13, 10.76. MALDI-TOF-MS *m/z*: [M^+] calculated for $C_{30}H_{24}Br_2O_2S_6$, 765.8; found, 765.3.

Poly{4,8-bis(5-(2-ethylhexyl)thiophen-2-yl)benzo[1,2-*b*:4,5-*b*']dithiophen-alt-2-(2-ethylhexyl)-5,7-bis(4-hexylthiophen-2-yl)benzo[1,2-*b*:4,5-*c*']dithiophene-4,8-dione} (**PBDT-AT**). The polymerization was performed by a Stille coupling reaction. In a 50 mL flask, **M1** (182 mg, 0.22 mmol) and **M3** (201 mg, 0.22 mmol) were dissolved in 10 mL toluene, and the solution was flushed with argon for 15 min, then 30 mg $Pd(PPh_3)_4$ was added into the solution. The mixture was again flushed with argon for 20 min. The reaction mixture was heated to reflux for 24 h. The reaction mixture was cooled to room temperature and added dropwise to 200 mL methanol. The precipitate was collected and further purified by Soxhlet extraction with methanol, hexane, and chloroform in sequence. The chloroform fraction was concentrated and added dropwise into methanol. Finally, the precipitates were collected and dried under vacuum overnight to get **PBDT-AT** as a purple solid (219 mg, yield 80%). ^{1}H NMR ($CDCl_3$, 400 MHz): δ (ppm) 7.78 (br, 3H), 7.43 (s, 1H), 7.38 (br, 3H), 6.94 (br, 2H), 2.90–2.85 (br, 10H), 1.73–1.23 (br, 43H), 1.17–1.08 (br, 24H). Elem. Anal. for $(C_{72}H_{86}O_2S_8)_n$ Calc: C, 69.63; H, 7.14; Found: C, 69.17; H, 7.18.

Poly{4,4-bis(2-ethylhexyl)-4H-silolo[3,2-*b*:4,5-*b*']dithiophene-alt-2-(2-ethylhexyl)-5,7-bis(4-hexylthiophen-2-yl)benzo[1,2-*b*:4,5-*c*']dithiophene-4,8-dione} (**PDTS-AT**). **PDTS-AT** was synthesized by following the same procedure for **PBDT-AT** but using **M5** instead of **M3. M1** (200 mg, 0.24 mmol) and **M5** (180 mg, 0.24 mmol) were used as starting materials in the polymerization. Finally, **PDTS-AT** was obtained as a black solid (104 mg, yield 40%). ^{1}H NMR ($CDCl_3$, 400 MHz): δ (ppm) 7.43 (br, 1H), 7.08–6.69 (br, 4H), 3.06–2.76 (br, 10H), 1.54–0.97 (br, 67H). Elem. Anal. for $(C_{62}H_{82}O_2S_6Si)_n$ Calc: C, 68.84; H, 7.83; Found: C, 66.18; H, 7.79.

Poly{4,8-bis(5-(2-ethylhexyl)thiophen-2-yl)benzo[1,2-*b*:4,5-*b*']dithiophen-alt-2-(2-ethylhexyl)-5,7-bis(thieno[3,2-b]thiophen-2-yl)benzo[1,2-*b*:4,5-*c*']dithiophene-4,8-dione} (**PBDT-TT**). **PBDT-TT** was synthesized by following the same procedure for **PBDT-AT. M2** (153 mg, 0.20 mmol) and **M4** (225 mg, 0.20 mmol) were used as starting materials. Finally, **PBDT-TT** was obtained as a black solid (197 mg, yield 69%). ^{1}H NMR ($CDCl_3$, 400 MHz): δ (ppm) 7.80–7.78 (br, 2H), 7.76–7.40 (br, 2H), 7.38–7.36 (br, 2H), 7.28 (br, 2H), 6.73 (br, 1H), 2.85 (br, 9H), 1.75–0.78 (br, 74H). Elem. Anal. for$(C_{80}H_{94}O_2S_{10})_n$ Calc: C, 68.13; H, 6.86; Found: C, 66.94; H, 6.67.

Poly{4,4′-bis(2-ethylhexyl)dithieno[3,2-*b*:2′,3′-*d*]silole-5,5′-diyl-alt-2-(2-ethylhexyl)-5,7-bis(thieno[3,2-*b*]thiophen-2-yl)benzo[1,2-*b*:4,5-*c*']dithiophene-4,8-dione} (**PDTS-TT**). **PDTS-TT** was synthesized by following the same procedure for **PBDT-AT. M2** (200 mg, 0.26 mmol) and **M5** (190 mg, 0.26 mmol) were used as starting materials. Finally, **PDTS-TT** was obtained as a black solid (93 mg, yield 35%). ^{1}H NMR ($CDCl_3$, 400 MHz): δ (ppm) 8.02 (br, 2 H), 7.43 (br, 1H), 7.08 (br, 2H), 6.72–6.70 (br, 2H), 2.96–2.69 (br, 6H), 1.54–0.87 (br, 45H). Elem. Anal. for $(C_{54}H_{58}O_2S_8Si)_n$ Calc: C, 63.24; H, 5.90; Found: C, 62.52; H, 5.87.

ACKNOWLEDGMENTS

This work was supported by the National Natural Science Foundation of China (21004050, 50933003), the General Program of the Education Department of Hunan Province (No.YB2011B030), and the Innovation Group and Xiangtan Joint Project in Hunan Natural Science Foundation (12JJ7002).

REFERENCES

1 (a) J. Chen, Y. Cao, *Acc. Chem. Res.* **2009**, *42*, 1709–1718; (b) P.-L. T. Boudreault, A. Najari, M. Leclerc, *Chem. Mater.* **2011**, *23*, 456–469; (c) Y. F. Li, *Acc. Chem. Res.* **2012**, *45*, 723–733; (d) H. Zhou, L. Yang, W. You, *Macromolecules* **2012**, *45*, 607–632; (e) C. Duan, F. Huang, Y. Cao, *J. Mater. Chem.* **2012**, *22*, 10416–10434; (f) H. J. Son, B. Carsten, I. H. Jung, L. Yu, *Energy Environ. Sci.* **2012**, *5*, 8158–8170; (g) Z.-G. Zhang, J. Wang, *J. Mater. Chem.* **2012**, *22*, 4178–4187.

2 (a) G. Yu, J. Gao, J. C. Hummelen, F. Wudl, A. J. Heeger, *Science* **1995**, *270*, 1789–1791; (b) J. Roncali, *Chem. Rev.* **1997**, *97*, 173–205.

3 (a) C. E. Small, S. Chen, J. Subbiah, C. M. Amb, S.-W. Tsang, T.-H. Lai, J. R. Reynolds, F. So, *Nat. Photonics* **2012**, *6*, 115–120; (b) M. X. Wang, Hu, P. Liu, W. Li, X. Gong, F. Huang, Y. Cao, *J. Am. Chem. Soc.* **2011**, *133*, 9638–9641; (c) E. Wang, Z. Ma, Z. Zhang, K. Vandewal, P. Henriksson, O. Inganäs, F. Zhang, M. R. Andersson, *J. Am. Chem. Soc.* **2011**, *133*, 14244–14247.

4 (a) H. C. Chen, Y. H. Chen, C. C. Liu, Y. C. Chien, S. W. Chou, P. T. Chou, *Chem. Mater.* **2012**, *24*, 4766–4772; (b) T. Y. Chu, J. Lu, S. Beaupré, Y. Zhang, J. R. Pouliot, S. Wakim, J. Zhou, M. Leclerc, Z. Li, J. Ding, Y. Tao, *J. Am. Chem. Soc.* **2011**, *133*, 4250–4253; (c) H. Zhou, L. Yang, A. C. Stuart, S. C. Price, S. Liu, W. You, *Angew. Chem. Int. Ed.* **2011**, *50*, 2995–2988; (d) L. Dou, W.-H. Chang, J. Gao, C.-C. Chen, J. You, Y. Yang, *Adv. Mater.* **2013**, *25*, 825–831; (e) C. Cabanetos, A. E. Labban, J. A. Bartelt,

J. D. Douglas, W. R. Mateker, J. M. J. Frechet, M. D. McGehee, P. M. Beaujuge, *J. Am. Chem. Soc.* **2013**, *134*, 4656; (f) X. Guo, M. Zhang, J. Tan, S. Zhang, L. Huo, W. Hu, Y. Li, J. Hou, *Adv. Mater.* **2012**, *24*, 6536–6541; (g) C. H. Cui, W.-Y. Wong, Y. F. Li, *Energy Environ. Sci.* **2014**; doi:10.1039/C4EE00446A.

5 J. You, L. Dou, K. Yoshimura, T. Kato, K. Ohya, T. Moriarty, K. Emery, C.-C. Chen, J. Gao, G. Li, Y. Yang, *Nat. Commun.* **2013**, *4*, 1446.

6 (a) X. C. Wang, S. Chen, Y. P. Sun, M. J. Zhang, Y. F. Li, X. Y. Li, H. Q. Wang, *Polym. Chem.* **2011**, *2*, 2872–2877; (b) M. J. Zhang, X. Guo, Y. F. Li, *Macromolecules* **2011**, *44*, 8798–8804; (c) N. S. Baek, S. K. Hau, H.-L. Yip, O. Acton, K.-S. Chen, A. K.-Y. Jen, *Chem. Mater.* **2008**, *20*, 5734–5736; (d) C. H. Woo, P. M. Beaujuge, T. W. Holcombe, O. P. Lee and J. M. J. Fréchet, *J. Am. Chem. Soc.* **2010**, *132*, 15547–15549; (e) J. Min, Z.-G. Zhang, S. Zhang, M. Zhang, J. Zhang, Y. Li, *Macromolecules* **2011**, *44*, 7632–7638; (f) X. Wang, Y. Sun, S. Chen, X. Guo, M. Zhang, X. Li, Y. Li, H. Wang, *Macromolecules* **2012**, *45*, 1208–1216; (g) X. Guo, M. Zhang, L. Huo, F. Xu, Y. Wu, J. Hou, *J. Mater. Chem.* **2012**, *22*, 21024–21031; (h) X. Ma, X. Mao, S. Zhang, X. Huang, Y. Cheng, C. Zhu, *Polym. Chem.* **2013**, *4*, 520–527; (i) X. Wang, P. Jiang, Y. Chen, H. Luo, Z. Zhang, H. Wang, X. Li, G. Yu, Y. Li, *Macromolecules* **2013**, *46*, 4805; (j) P. M. Beaujuge, W. Pisula, H. N. Tsao, S. Ellinger, K. Mullen, J. R. Reynolds, *J. Am. Chem. Soc.* **2009**, *131*, 7514–7515. (k) F. Huang, K.-S. Chen, H.-L. Yip, S. K. Hau, O. Acton, Y. Zhang, J. D. Luo, A. K.-Y. Jen, *J. Am. Chem. Soc.* **2009**, *131*, 13886–13887; (l) S. Subramaniyan, H. Xin, F. S. Kim, S. A. Jenekhe, *Macromolecules* **2011**, *44*, 6245–6248; (m) C. L. Chochos, S. A. Choulis, *Prog. Polym. Sci.* **2011**, *36*, 1326–1414.

7 (a) L. Huo, J. Hou, S. Zhang, H.-Y. Chen, Y. Yang, *Angew. Chem.* **2010**, *122*, 1542–1545; (b) L. Huo, S. Zhang, X. Guo, F. Xu, Y. Li, J. Hou, *Angew. Chem. Int. Ed.* **2011**, *50*, 9697–9702; (c) Y. Huang, X. Guo, F. Liu, L. Huo, Y. Chen, T. P. Russell, C. C. Han, Y. Li, J. Hou, *Adv. Mater.* **2012**, *24*, 3383–3389; (d) R. Duan, L. Ye, X. Guo, Y. Huang, P. Wang, S. Zhang, J. Zhang, L. Huo, J. Hou, *Macromolecules* **2012**, *45*, 3032–3038.

8 (a) H. Bronstein, Z. Chen, R. S. Ashraf, W. Zhang, J. Du, J. R. Durrant, P. S. Tuladhar, K. Song, S. E. Watkins, Y. Geerts, M. M. Wienk, R. A. J. Janssen, T. Anthopoulos, H. Sirringhaus, M. Heeney, I. McCulloch, *J. Am. Chem. Soc.* **2011**, *133*, 3272; (b) P. Liu, Y. L. Wu, H. L. Pan, Y. N. Li, S. Gardner, B. S. Ong, S. P. Zhu, *Chem. Mater.* **2009**, *21*, 2727–2732; (c) X. G. Guo, F. S. Kim, M. J. Seger, S. A. Jenekhe, M. D. Watson, *Chem. Mater.* **2012**, *24*, 1434–1442; (d) M. Al-Hashimi, J. G. Labram, S. Watkins, M. Motevalli, T. D. Anthopoulos, M. Heeney, *Org. Lett.* **2010**, *12*, 5748; (e) J. S. Lee, S. K. Son, S. Song, H. Kim, D. R. Lee, K. Kim, M. J. Ko, D. H. Choi, B. Kim, J. H. Cho, *Chem. Mater.* **2012**, *24*, 1316–1323; (f) Z. Chen, M. J. Lee, R. S. Ashraf, Y. Gu, S. Albert-Seifried, M. M. Nielsen, B. Schroeder, T. D. Anthopoulos, M. Heeney, I. McCulloch, H. Sirringhaus, *Adv. Mater.* **2012**, *24*, 647–652.

9 J. Cao, W. Zhang, Z. Xiao, L. Liao, W. Zhu, Q. Zuo, L. Ding, *Macromolecules* **2012**, *45*, 1710–1714.

10 (a) Y. Ie, J. Huang, Y. Uetani, M. Karakawa, Y. Aso, *Macromolecules* **2012**, *45*, 4564–4571; (b) D. Qian, L. Ye, M. Zhang, Y. Liang, L. Li, Y. Huang, X. Guo, S. Zhang, Z. Tan, J. Hou, *Macromolecules* **2012**, *45*, 9611–9617.

11 H. Usta, G. Lu, A. Facchetti, T. J. Marks, *J. Am. Chem. Soc.* **2006**, *128*, 9034–9035.

12 J. Pommerehne, H. Vestweber, W. Guss, R. F. Mahrt, H. Bassler, M. Porsch, J. Daub, *Adv. Mater.* **1995**, *7*, 551–554.

13 (a) C.-J. Yang, S. A. Jenekhe, *Macromolecules* **1995**, *28*, 1180–1196; (b) P.-T. Wu, T. Bull, F. S. Kim, C. K. Luscombe, S. A. Jenekhe, *Macromolecules* **2009**, *42*, 671–681; (c) W. C. Chen, C. L. Liu, C. T. Yen, F. C. Tasi, C. J. Tonzola, N. Olson, S. A. Jenekhe, *Macromolecules* **2004**, *37*, 5959–5964.

14 Y. J. He, Y. F. Li, *Phys. Chem. Chem. Phys.* **2011**, *13*, 1970–1983.

15 B.C. Thompson, Y.G. Kim, J. R. Reynolds, *Macromolecules* **2005**, *38*, 5359–5362.

16 (a) J. Li, K.-H. Ong, P. Sonar, S.-L. Lim, G.-M. Ng, H.-K. Wong, H.-S. Tan, Z.-K. Chen, *Polym. Chem.* **2013**, *4*, 804; (b) K. Vandewal, K. Tvingstedt, A. Gadisa, O. Inganäs, J. V. Manca, *Nat. Mater.* **2009**, *8*, 904–909; (c) J. Y. Kim, Y. Qin, D. M. Stevens, O. Ugurlu, V. Kalihari, M. A. Hillmyer, C. D. Frisbie, *J. Phys. Chem. C* **2009**, *113*, 10790–10797; (d) D. Veldman, O. İpek, S. C. J. Meskers, J. Sweelssen, M. M. Koetse, S. C. Veenstra, J. M. Kroon, S. S. Bavel, J. Loos, R. A. J. Janssen, *J. Am. Chem. Soc.* **2008**, *130*, 7721–7735.

17 (a) X. Liu, W. Wen, G. C. Bazan, *Adv. Mater.* **2012**, *24*, 4505–4510; (b) H. Li, H. W. Tang, L. G. Li, W. T. Xu, X. L. Zhao, X. N. Yang, *J. Mater. Chem.* **2011**, *21*, 6563–6568; (c) S. Nam, J. Jang, H. Cha, J. Hwang, T. K. An, S. Park, C. E. Park, *J. Mater. Chem.* **2012**, *22*, 5543–5549; (d) Q. Wang, Y. Zhou, H. Zheng, J. Shi, C. Z. Li, C. M. Q. Su, L. Wang, C. Luo, D. G. Hu, J. Pei, J. Wang, J. B. Peng, Y. Cao, *Org. Electron.* **2011**, *12*, 1858–1863; (e) H. Zhou, Y. Zhang, J. Seifter, S. D. Collins, C. Luo, G. C. Bazan, T.-Q. Nguyen, A. J. Heeger, *Adv. Mater.* **2013**, *25*, 1646–1652; (f) Y. Wang, Y. Liu, S. Chen, R. Peng, Z. Ge, *Chem. Mater.* **2013**, *25*, 3196.

18 (a) M. D. Perez, C. Borek, S. R. Forrest, M. E. Thompson, *J. Am. Chem. Soc.* **2009**, *131*, 9281–9286; (b) K. Vandewal, K. Tvingstedt, A. Gadisa, O. Inganäs, J. V. Manca, *Nat. Mater.* **2009**, *8*, 904–909; (c) L. Yang, H. Zhou, W. You, *J. Phys. Chem. C* **2010**, *114*, 16793–16800.

19 G. G. Malliaras, J. R. Salem, P. J. Brock, C. Scott, *Phys. Rev. B: Condens. Matter* **1998**, *58*, 13411–13414.

20 (a) X. Liu, J. Zhang, P. Tang, G. Yu, Z. Zhang, H. Chen, Y. Chen, B. Zhao, S. Tan, P. Shen, *Org. Electron.* **2012**, *13*, 1671–1679; (b) H. Chen, Y. Guo, G. Yu, Y. Zhao, J. Zhang, D. Gao, H. Liu, Y. Liu, *Adv. Mater.* **2012**, *24*, 4618–4622; (c) H. N. Tsao, D. M. Cho, I. Park, M. R. Hansen, A. Mavrinskiy, D. Y. Yoon, R. Graf, W. Pisula, H. W. Spiess, K. Müllen, *J. Am. Chem. Soc.* **2011**, *133*, 2605–2611.

21 P. Shen, B. Zhao, X. Huang, H. Huang, S. Tan, *Eur. Polym. J.* **2009**, *45*, 2726–2731.